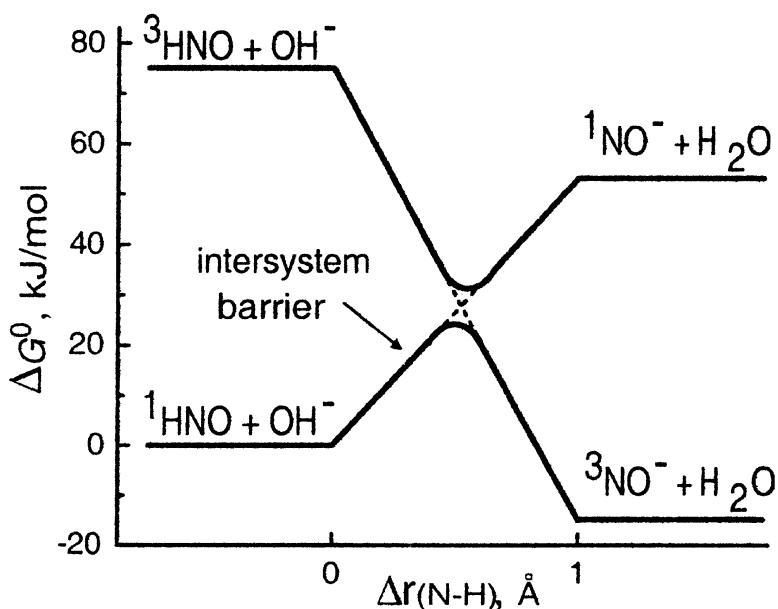


Spin-Forbidden Deprotonation of Aqueous Nitroxyl (HNO)

Vladimir Shafirovich, and Sergei V. Lyman

J. Am. Chem. Soc., **2003**, 125 (21), 6547-6552 • DOI: 10.1021/ja034378j • Publication Date (Web): 01 May 2003

Downloaded from <http://pubs.acs.org> on March 28, 2009



More About This Article

Additional resources and features associated with this article are available within the HTML version:

- Supporting Information
- Links to the 3 articles that cite this article, as of the time of this article download
- Access to high resolution figures
- Links to articles and content related to this article
- Copyright permission to reproduce figures and/or text from this article

[View the Full Text HTML](#)



ACS Publications
 High quality. High impact.

Spin-Forbidden Deprotonation of Aqueous Nitroxyl (HNO)

Vladimir Shafirovich[†] and Sergei V. Lyamar^{*‡}*Contribution from the Chemistry Department and Radiation and Solid State Laboratory, New York University, New York, New York 10003 and Chemistry Department, Brookhaven National Laboratory, Upton, New York 11973*

Received January 28, 2003; E-mail: lyamar@bnl.gov

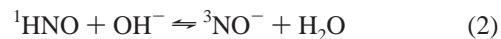
Abstract: The first mechanistic study of a spin-forbidden proton-transfer reaction in aqueous solution is reported. Laser flash photolysis of alkaline trioxodinitrate ($\text{N}_2\text{O}_3^{2-}$, Angeli's anion) is used to generate a nitroxyl anion in its excited singlet state ($^1\text{NO}^-$). Through rapid partitioning between protonation by water and electronic relaxation, $^1\text{NO}^-$ produces ^1HNO (ground state, yield 96%) and $^3\text{NO}^-$ (ground state, yield 4%), which comprise a unique conjugate acid–base couple with different ground-state multiplicities. Using the large difference between reactivities of ^1HNO and $^3\text{NO}^-$ in the peroxyxynitrite-forming reaction with $^3\text{O}_2$, the kinetics of spin-forbidden deprotonation reaction $^1\text{HNO} + \text{OH}^- \rightarrow ^3\text{NO}^- + \text{H}_2\text{O}$ is investigated in H_2O and D_2O . Consistent with proton transfer, this reaction exhibits primary kinetic hydrogen isotope effect $k(\text{H})/k(\text{D}) = 3.1$ at 298 K, which is found to be temperature-dependent. Arrhenius pre-exponential factors and activation energies of the second-order rate constant are found to be: $\log(A, \text{M}^{-1} \text{s}^{-1}) = 10.0 \pm 0.2$ and $E_a = 30.0 \pm 1.1 \text{ kJ/mol}$ for proton transfer and $\log(A, \text{M}^{-1} \text{s}^{-1}) = 10.4 \pm 0.1$ and $E_a = 35.1 \pm 0.7 \text{ kJ/mol}$ for deuteron transfer. Collectively, these data are interpreted to show that the nuclear reorganization requirements arising from the spin prohibition necessitate significant activation before spin change can take place, but the spin change itself must occur extremely rapidly. It is concluded that a synergy between the spin prohibition and the reaction energetics creates an intersystem barrier and is responsible for slowness of the spin-forbidden deprotonation of ^1HNO by OH^- ; the spin prohibition alone plays a minor role.

Introduction

Nitroxyl (HNO, with the hydrogen atom on the nitrogen atom) is the protonated one-electron reduction product of the nitric oxide ($\text{NO}\cdot$) radical and can be produced by radiation in a variety of NO-rich environments, including certain types of nuclear wastes. Conceivably, nitroxyl can also be generated in biological systems either en route to $\text{NO}\cdot$ from various sources or as an intermediate of $\text{NO}\cdot$ metabolism. These possibilities have attracted considerable interest and have been the subject of several recent investigations.^{1–6} The data interpretations and the evaluations of biological roles of nitroxyl have invariably invoked its chemical properties and reactivity, which are not well-understood and remain controversial despite the apparent simplicity of the molecule.

One highly unusual and not always properly recognized complication in dealing with nitroxyl is that its conjugate anion (NO^-), which is isoelectronic with molecular oxygen, has a

triplet ground state ($^3\Sigma^-$), whereas the ground state of HNO is a singlet ($^1A'$). These properties make the acid–base equilibria



spin-forbidden and inherently slow. Recently, we have shown that the reactivity pattern of HNO/ NO^- species toward O_2 and $\text{NO}\cdot$ is fully consistent with these ground-state assignments and have estimated $\text{p}K_a(^1\text{HNO}/^3\text{NO}^-) \approx 11.4$ for the ground state ($^1A'$) to ground state ($^3\Sigma^-$) acid dissociation and $\text{p}K_a(^1\text{HNO}/^1\text{NO}^-) \approx 23$ for the ground state ($^1A'$) to excited state ($^1\Delta$) acid dissociation;⁷ very similar $\text{p}K_a$ values have been obtained by Fukuto, Houk, and co-workers.⁸ These assessments suggest that HNO is a much weaker acid than it was previously believed based on the widely accepted $\text{p}K_a(\text{HNO}/\text{NO}^-) = 4.7$ derived some 30 years ago from pulse radiolysis experiments by Grätzel and co-workers⁹ and presumably pertaining to the ground states, although the spin states were not considered at all in that work. One important implication of the $\text{p}K_a$ re-evaluation is that ^1HNO , but not $^3\text{NO}^-$ or $^1\text{NO}^-$, is the dominant form of nitroxyl

[†] Chemistry Department and Radiation and Solid State Laboratory, New York University.

[‡] Chemistry Department, Brookhaven National Laboratory.

- (1) Wong, P. S. Y.; Hyun, J.; Fukuto, J. M.; Shiota, F. N.; DeMaster, E. G.; Shoeman, D. W.; Nagasawa, H. T. *Biochemistry* **1998**, *37*, 5362–5371.
- (2) Adak, S.; Wang, Q.; Stuehr, D. J. *J. Biol. Chem.* **2000**, *275*, 33554–33561.
- (3) Miranda, K. M.; Espey, M. G.; Yamada, K.; Krishna, M.; Ludwick, N.; Kim, S.; Jourdeuil, D.; Grisham, M. B.; Feelisch, M.; Fukuto, J. M.; Wink, D. A. *J. Biol. Chem.* **2001**, *276*, 1720–1727.
- (4) Reif, A.; Zecca, L.; Riederer, P.; Feelisch, M.; Schmidt, H. *Free Radic. Biol. Med.* **2001**, *30*, 803–808.
- (5) Kirsch, M.; de Groot, H. *J. Biol. Chem.* **2002**, *277*, 13379–13388.
- (6) Liochev, S. I.; Fridovich, I. *Arch. Biochem. Biophys.* **2002**, *402*, 166–171.

(7) Shafirovich, V.; Lyamar, S. V. *Proc. Natl. Acad. Sci. U.S.A.* **2002**, *99*, 7340–7345.

(8) Bartberger, M. D.; Liu, W.; Ford, E.; Miranda, K. M.; Switzer, C.; Fukuto, J. M.; Farmer, P. J.; Wink, D. A.; Houk, K. N. *Proc. Natl. Acad. Sci. U.S.A.* **2002**, *99*, 10958–10963.

(9) Grätzel, M.; Taniguchi, S.; Henglein, A. *Ber. Bunsen-Ges. Phys. Chem.* **1970**, *74*, 1003–1010.

under physiological conditions. On the other hand, if ${}^3\text{NO}^-$ is produced by some means in neutral or alkaline solution, it will persist for a sufficiently long time (several milliseconds according to our estimate)⁷ to engage in other reactions, e.g., with O_2 or $\text{NO}\cdot$, before undergoing spin-forbidden equilibration with ${}^1\text{HNO}$.

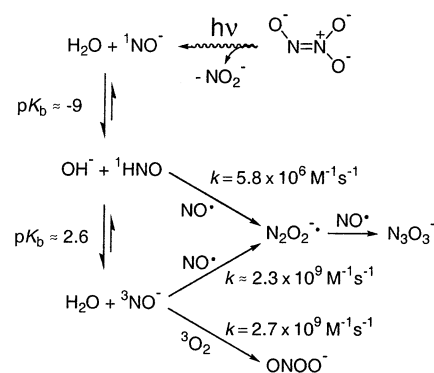
Conjugate acid–base couples with different ground-state multiplicities are rare in chemistry and so is the opportunity to investigate attendant spin-forbidden proton-transfer reactions. The handful of examples that we have found in the literature consist of gas-phase protonation of a distonic carbene ion by phenols,¹⁰ gas-phase protonation of ${}^3\text{NO}^-$ by certain acids,^{11,12} and protic equilibration of a stable organic biradical with organic acid or bases in acetonitrile.¹³ Within aqueous main-group chemistry, nitroxyl is likely to represent a unique instance of an acid whose dissociation and reactions with bases are spin-forbidden. In this study, we inquire into the nature and the mechanistic implications of spin restrictions in reaction 2 primarily through the measurements of its activation parameters and kinetic hydrogen isotope effect. We show that the nuclear reorganization (activation) requirements arising from the spin prohibition are more important in impeding this reaction than the spin prohibition per se.

Experimental Section

Sample Solutions. All chemicals of analytical grade and heavy water were used as received. Normal water (ASTM type I) was obtained from a Milli-Q purification system. The 0.15 mM stock solutions of Angeli's salt (sodium trioxodinitrate, $\text{Na}_2\text{N}_2\text{O}_3$, from Cayman Chemical) in 0.25 M NaOH or NaOD were prepared daily and used within 2–3 h. Nitric oxide (Matheson) was purified from N_2O_3 by passing the gas through a scrubbing column with 2 M KOH and then through water. All solutions were thoroughly purged with argon prior to introducing nitric oxide. Oxygen gas was used as received. Only saturated solutions of $\text{NO}\cdot$ or O_2 were used and their concentrations taken as 1.9 and 1.3 mM, respectively, were always in large excess over photochemically generated nitroxyl species.

Kinetic Measurements. Transient kinetics were recorded using a fully computerized laser flash photolysis system with the right angle cross-beam arrangement in a massive quartz flow cell (depth 0.4 cm, length 1 cm, illuminated volume 0.16 mL) as described elsewhere.^{7,14} Solution of $\text{N}_2\text{O}_3^{2-}$ saturated with a desired gas in the feed reservoir was forced by a positive gas pressure into the cell through a computer-controlled solenoid valve. A 266 nm Nd:YAG laser (typical pulse energy 30–40 mJ/cm²) was used to photolyze the samples. A computer-controlled shutter on the laser beam was employed to select individual excitation pulses from a 20 Hz laser pulse train. The transient absorption was probed along a 1 cm optical path by a light beam from a 75 W xenon arc lamp (pulsed for short time scales) and the kinetic traces obtained were averaged over 10 laser pulses. For the measurements of temperature dependencies, the flow cell was thermostated within a copper holder equipped with a circulating water jacket. To allow for solution replacement and thermal stabilization between the laser shots, the following automated protocol was employed: rinse and refill the cell, wait 2 min for the solution temperature stabilization, execute 1 laser shot and data acquisition, repeat.

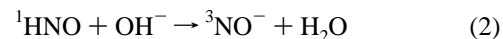
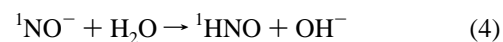
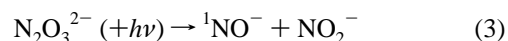
Scheme 1



Results

The experimental design of this work is entirely based on our recent investigation of the reactivity of HNO/NO^- species toward O_2 and $\text{NO}\cdot$.⁷ Pertinent mechanistic information obtained in that study is summarized by Scheme 1 showing the relationship between various forms of nitroxyl and their reactions that are used here.

Photochemical cleavage of the trioxodinitrate dianion ($\text{N}_2\text{O}_3^{2-}$), which can be viewed as a stable N–N adduct between NO^- and NO_2^- , provides a convenient method to rapidly generate nitroxyl species. In strongly alkaline solutions, successive formation of several nitroxyl species has been assigned to the following reactions initiated by UV laser light⁷



The photochemical step and the protonation of ${}^1\text{NO}^-$ by water are both extremely rapid, whereas the spin-forbidden reaction 2 is comparatively slow. Due to insufficient absorption in the accessible spectral range by both ${}^1\text{HNO}$ and ${}^3\text{NO}^-$, this reaction could not be monitored directly. However, the appearance of ${}^3\text{NO}^-$ in solution due to reaction 2 can be visualized in the presence of oxygen through the formation of peroxynitrite (ONOO^- , $\lambda_{\text{max}} = 302$ nm, $\epsilon_{302} = 1670$ M⁻¹ cm⁻¹), i.e., the reaction



which is nearly diffusion-controlled ($k_6 = 2.7 \times 10^9$ M⁻¹ s⁻¹).⁷ The observed first-order rate constant for peroxynitrite accumulation is independent of oxygen concentration in the 0.035–1.3 mM range and is proportional to the hydroxide ion concentration⁷

$$k_{\text{obs}} = k_2[\text{OH}^-] \quad (7)$$

From this and other evidence, it has been concluded that reaction 2 is the rate-determining step in the reaction sequence 3, 4, 2, and 6 leading to peroxynitrite accumulation.⁷

Typical kinetics of peroxynitrite accumulation following flash photolysis of O_2 -saturated solutions of $\text{N}_2\text{O}_3^{2-}$ in H_2O and D_2O are shown in Figure 1. The kinetic traces were monitored at 315 nm to minimize interference from the prompt bleaching of

(10) Hu, J.; Hill, B. T.; Squires, R. R. *J. Am. Chem. Soc.* **1997**, *119*, 11699–11700.

(11) Janaway, G. A.; Zhong, M.; Gatev, G. G.; Chabinyk, M. L.; Brauman, J. I. *J. Am. Chem. Soc.* **1997**, *119*, 11697–11698.

(12) Janaway, G. A.; Brauman, J. I. *J. Phys. Chem. A* **2000**, *104*, 1795–1798.

(13) Ishiguro, K.; Ozaki, M.; Sekine, N.; Sawaki, Y. *J. Am. Chem. Soc.* **1997**, *119*, 3625–3626.

(14) Shafirovich, V.; Dourandin, A.; Huang, W.; Luneva, N. P.; Geacintov, N. E. *J. Phys. Chem. B* **1999**, *103*, 10924–10933.

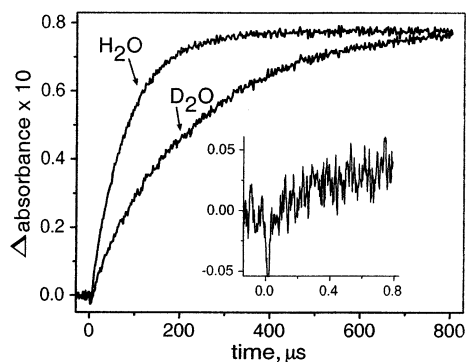


Figure 1. Kinetic traces of ONOO⁻ accumulation recorded at 315 nm after flash photolysis of 0.15 mM N₂O₃²⁻ in O₂-saturated H₂O (upper trace) and D₂O (lower trace) solutions containing 0.25 M NaOH and 0.25 M NaOD, respectively. Inset shows the first microsecond portion of the kinetics in H₂O; the short negative-going signal at the time origin is due to laser stray light.

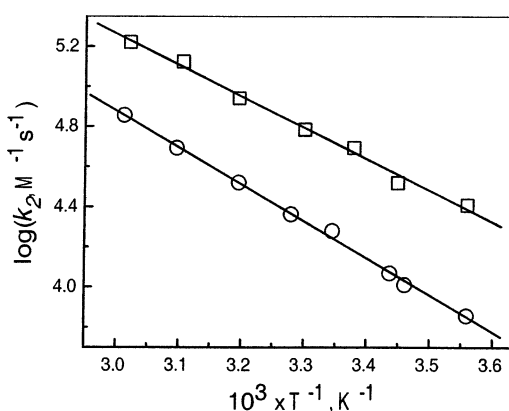


Figure 2. Temperature dependencies of the bimolecular rate constants for deprotonation of ¹HNO by OH⁻ (reaction 2) in H₂O (squares) and in D₂O (circles). The lines give linear fits to the data points. Solution compositions are identical with those in Figure 1.

Table 1. Arrhenius Activation Parameters^a for the Second-Order Rate Constant of Reaction 2

solvent	log(A ₂ , M ⁻¹ s ⁻¹)	E _a , kJ/mol	k ₂ (298 K), M ⁻¹ s ⁻¹
H ₂ O ^b	10.0 ± 0.2	30.0 ± 1.1	5.5 × 10 ⁴
D ₂ O ^c	10.4 ± 0.1	35.1 ± 0.7	1.8 × 10 ⁴

^a Uncertainties are given as standard errors for the linear fits in Figure 2. ^b In 0.25 M NaOH. ^c In 0.25 M NaOD.

N₂O₃²⁻ absorption (λ_{max} = 248 nm, ε₂₄₈ = 8300 M⁻¹ cm⁻¹) induced by the laser flash. It is evident from Figure 1 that, although the peroxyxynitrite signal amplitudes at the end of the kinetic runs are practically identical in H₂O and D₂O, there is a significant and normal kinetic isotope effect, that is k_{obs}(H₂O) > k_{obs}(D₂O). The temperature dependencies of k_{obs} in the 8–60 °C range have been measured at constant 0.25 M alkali concentrations and the corresponding bimolecular rate constants k₂ (eq 7) are plotted in Figure 2. Arrhenius parameters derived from these plots are given in Table 1. The kinetic isotope effect was found to be weakly temperature-dependent and KIE = k₂(H₂O)/k₂(D₂O) = 3.1 at 298 K. The magnitude of KIE is characteristic of primary isotope effect,^{15,16} which is also

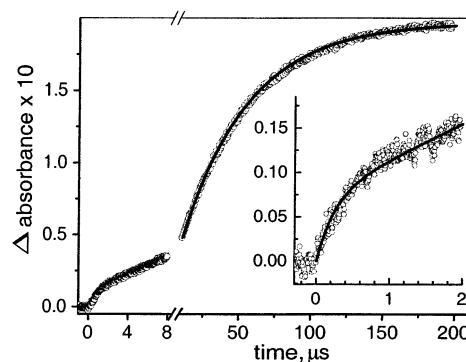


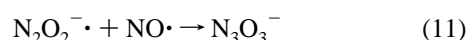
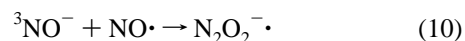
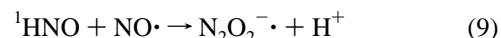
Figure 3. Kinetic traces of N₃O₃⁻ accumulation recorded at 380 nm after flash photolysis of 0.15 mM N₂O₃²⁻ in NO-saturated H₂O solution containing 0.25 M NaOH; note the time axis break at 8.5 μs. Inset shows the first 2 μs portion of the kinetics. The traces are from separate kinetic runs on 3 different time scales. Solid lines correspond to eq 12 with ΔA_{fast} = 0.0073, k_{fast} = 4.0 × 10⁶ s⁻¹, ΔA_{slow} = 0.19, and k_{slow} = 2.2 × 10⁴ s⁻¹.

consistent with the proton-transfer reaction 2 being the rate-limiting step.

There is a very small but reproducible rise of the peroxyxynitrite absorption occurring within one microsecond after the laser flash (Figure 1, inset). Although this rise corresponds to less than 5% of the total accumulation of ONOO⁻, it can be mechanistically important because it suggests that a small amount of ³NO⁻ is present in solution immediately after the laser pulse. Indeed, the expected characteristic rise time of ONOO⁻ from reaction 6 is about 0.3 μs in O₂-saturated solution. Thus, the inset in Figure 1 can be interpreted as indicating that there is a partitioning between protonation of ¹NO⁻ by water (reaction 4) and its intersystem crossing to the ground state



This partitioning of ¹NO⁻ has been determined more quantitatively by replacing O₂ with NO[•]. In this case (Scheme 1), the long-lived strongly absorbing N₃O₃⁻ ion (λ_{max} = 380 nm, ε₃₈₀ ≈ 4000 M⁻¹ cm⁻¹) is produced from both ¹HNO and ³NO⁻ by consecutive addition of two NO[•] radicals in the following reactions^{7,9,17}



Reaction 9 is relatively slow (k₉ = 5.8 × 10⁶ M⁻¹ s⁻¹), whereas both reactions 10 and 11 are essentially diffusion-controlled.⁷ The kinetics of N₃O₃⁻ accumulation in NO-saturated solution is shown in Figure 3, where the rapid step of product formation is seen much more clearly than with ONOO⁻.

The overall kinetics conforms a two-exponential growth

$$\Delta A_t = \Delta A_{\text{fast}} \{1 - \exp(-k_{\text{fast}} t)\} + \Delta A_{\text{slow}} \{1 - \exp(-k_{\text{slow}} t)\} \quad (12)$$

where ΔA_{fast} and ΔA_{slow} are the absorption amplitudes and k_{fast} and k_{slow} are the first-order rate constants for the fast and slow steps, respectively. Simultaneous fitting of all traces in Figure

(15) More O'Ferrall, R. A. In *Proton-Transfer Reactions*; Caldin, E., Gold, V., Eds.; Chapman and Hall: London, 1975; pp 201–262.

(16) Hibbert, F. In *Comprehensive Chemical Kinetics*; Bamford, C. H., Tipper, C. F. H., Eds.; Elsevier: Amsterdam, 1977; Vol. 8, pp 97–196.

(17) Seddon, W. A.; Fletcher, J. W.; Sopchysyn, F. C. *Can. J. Chem.* **1973**, *51*, 1123–1130.

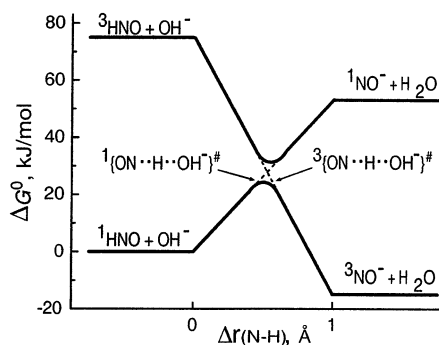


Figure 4. Free energy change drawn to scale for various reactions of the ${}^1\text{HNO} + \text{OH}^-$ couple in water. Solid lines approximate adiabatic energy profiles along the N–H distance change during proton transfer, $\Delta r(\text{N-H})$, that is shown as a reaction coordinate.

3 to eq 12 yielded $\Delta A_{\text{fast}} = 0.0073$, $k_{\text{fast}} = 4.0 \times 10^6 \text{ s}^{-1}$, $\Delta A_{\text{slow}} = 0.19$, and $k_{\text{slow}} = 2.2 \times 10^4 \text{ s}^{-1}$. The slow step corresponds to parallel occurrence of two reaction sequences 9, 11 and 2, 10, 11; its rate constant is $k_{\text{slow}} = k_9[\text{NO}\cdot] + k_2[\text{OH}^-]$. As with ONOO^- , the fast step can be interpreted as originating from a small amount of ${}^3\text{NO}^-$ that has been very rapidly produced by reaction 8; this interpretation is valid if $k_4 + k_8 \gg 1 \times 10^7 \text{ s}^{-1}$ and $k_4 \gg k_8$. We have previously reported the apparent rate constant of N_3O_3^- formation through reactions 10 and 11 in NO-saturated solution to be $4.3 \times 10^6 \text{ s}^{-1}$.⁷ This value is in good agreement with k_{fast} obtained by fitting kinetic traces in Figure 3 and the rapid yield of ${}^3\text{NO}^-$ through intersystem crossing is

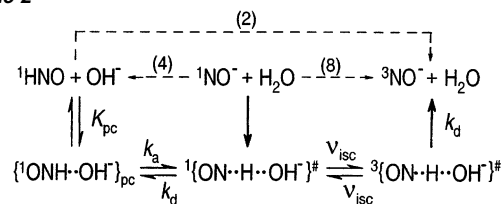
$$Y_{\text{isc}} = \Delta A_{\text{fast}} / (\Delta A_{\text{slow}} + \Delta A_{\text{fast}}) = k_8 / (k_4 + k_8) \approx 0.04 \quad (13)$$

Discussion

All oxygen and nitrogen acids without an intramolecular hydrogen bond belong to the so-called “normal acids”, for which proton transfer in the $\text{AH} + \text{B}^-$ reaction approaches diffusion-controlled rate, when the acidity difference $\text{p}K_{\text{a}}(\text{BH}) - \text{p}K_{\text{a}}(\text{AH})$ becomes greater than 2–3 units.^{16,18} By this criterion alone, reaction 2 should be about 5 orders of magnitude more rapid than observed. Somewhat surprisingly, its pre-exponential factor is within the range of those expected for a spin-allowed and otherwise uninhibited bimolecular reaction and so the low rate of reaction 2 is mostly associated with significant activation energy (Table 1). The necessity for activation in this reaction becomes clear from considering the energy diagram for reactants and products shown in Figure 4.

The diagram is based on the estimates for the Gibbs free energies of formation of aqueous nitroxyl species that we have reported previously⁷ and the tabulated values for water species.¹⁹ Complete proton transfer from HNO to OH^- should be accompanied by about 1 Å change in the N–H distance, which corresponds to the typical difference in the N–H distances for N–H···O and N···H–O hydrogen-bonded structural motifs.²⁰ Because of the spin restrictions, there is no barrierless route from reactants to products in reaction 2, as there would be for a “normal” acid–base reaction, and the encounter pair between

Scheme 2



${}^1\text{HNO}$ and OH^- must “climb” up to at least the intersection region of singlet and triplet energy surfaces in Figure 4 before the intersystem crossing can occur.

Such a mechanism is shown in Scheme 2, where the solid arrows indicate actual elementary reaction steps and the dashed arrows relate these steps to net reactions 2, 4, and 8. According to this mechanism, the intersystem crossing happens with frequency ν_{isc} in the activated complex $\{ \text{ON}\cdot\cdot\text{H}\cdot\cdot\text{OH} \}^\ddagger$ that has a nuclear configuration corresponding to the singlet–triplet intersection in Figure 4 and a lifetime corresponding to the classical reaction frequency, that is $k_{\text{d}} = RT/Nh \approx 6.2 \times 10^{12} \text{ s}^{-1}$.

As shown in Scheme 2, net reaction 8 can be interpreted as being water-assisted and proceeding through the same activated complex with net reactions 2 and 4. The small yield of ${}^3\text{NO}^-$ from ${}^1\text{NO}^-$ indicates that $k_{\text{d}} \gg \nu_{\text{isc}}$ and, from $Y_{\text{isc}} = \nu_{\text{isc}} / (k_{\text{d}} + \nu_{\text{isc}}) = 0.04$ (eq 13), we estimate $\nu_{\text{isc}} \approx 2.5 \times 10^{11} \text{ s}^{-1}$, i.e., the frequency of isoenergetic oscillations between singlet and triplet states in the activated complex must be very high. Such a facile transition can be qualitatively explained provided that the activated complex retains much of the reactant molecular orbital configuration. Indeed, HNO is analogous to a carbonyl in that it is isoelectronic with formaldehyde and its HOMO and LUMO are n and π^* , respectively. Then the ${}^1\{ \text{ON}\cdot\cdot\text{H}\cdot\cdot\text{OH} \}^\ddagger \rightarrow {}^3\{ \text{ON}\cdot\cdot\text{H}\cdot\cdot\text{OH} \}^\ddagger$ intersystem crossing involves the isoenergetic ${}^1(n, n) \rightarrow {}^3(n, \pi^*)$ molecular orbital change, which is allowed by El-Sayed’s selection rules.²¹ Such transitions, particularly in carbonyls, can occur at 10^{11} s^{-1} and even faster.^{21–24}

With $k_{\text{d}} \gg \nu_{\text{isc}}$, the overall activation-controlled rate constant for reaction 2 is

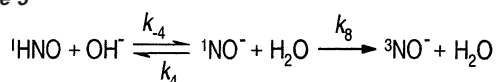
$$k_2 = K_{\text{pc}} K^\ddagger \nu_{\text{isc}} = K_{\text{pc}} \nu_{\text{isc}} \exp\left(\frac{\Delta S^\ddagger}{R}\right) \exp\left(-\frac{\Delta H^\ddagger}{RT}\right) \quad (14)$$

where K_{pc} (in M^{-1}) is the equilibrium constant for the formation of precursor complex with proper orientation and $K^\ddagger = k_{\text{a}}/k_{\text{d}}$, ΔS^\ddagger and ΔH^\ddagger are the activation equilibrium constant and the activation entropy and enthalpy, respectively. As there is no Coulombic interaction between ${}^1\text{HNO}$ and OH^- , the value of K_{pc} should be practically temperature-independent and determined mainly by the negative entropy of bringing these species together. Taking 2.9 Å for the N–O distance in the precursor complex, a typical value for the N–H···O hydrogen-bonded species,²⁰ and applying the procedure described by Creutz and Sutin,²⁵ we calculate $K_{\text{pc}} \approx 1.3 \times 10^{-2} \text{ M}^{-1}$. Therefore, $K_{\text{pc}} \nu_{\text{isc}} \approx 3.3 \times 10^9 \text{ M}^{-1} \text{ s}^{-1}$ and a small positive ΔS^\ddagger of the order of

(18) Crooks, J. E. In *Comprehensive Chemical Kinetics*; Bamford, C. H., Tipper, C. F. H., Eds.; Elsevier: Amsterdam, 1977; Vol. 8, pp 197–250.
 (19) Wagman, D. D.; Evans, W. H.; Parker, V. B.; Schumm, R. H.; Halow, I.; Bailey, S. M.; Churney, K. L.; Nuttall, R. L. *J. Phys. Chem. Ref. Data* **1982**, *11*, Suppl. 2.
 (20) Hamilton, W. C.; Ibers, J. A. *Hydrogen Bonding in Solids*; Benjamin: New York, 1968.

(21) Turro, N. J. *Modern Molecular Photochemistry*; Benjamin/Cummings: Menlo Park, California, 1978.
 (22) Damschen, D. E.; Merritt, C. D.; Perry, D. L.; Scott, G. W.; Talley, L. D. *J. Phys. Chem.* **1978**, *82*, 2268–2272.
 (23) Murov, S. L.; Carmichael, I.; Hug, G. L. *Handbook of Photochemistry*; Marcel Dekker: New York, 1993.
 (24) Singh, A. K.; Bhasikuttan, A. C.; Palit, D. K.; Mittal, J. P. *J. Phys. Chem. A* **2000**, *104*, 7002–7009.

Scheme 3



10 J/(mol K) would be sufficient to account for the observed pre-exponential factor in Table 1.

Although the value of $\Delta H^\ddagger = E_a$ cannot be predicted, except that it should be significantly positive, we note that the singlet–triplet intersection obtained by simple linear interpolation in Figure 4 occurs at 28 kJ/mol, which is remarkably close to the experimental $E_a = 30$ kJ/mol in Table 1. The observed isotope effect on E_a is explicable by the zero-point energy difference for the H–NO and D–NO stretching vibrations. The corresponding frequency difference ranging from 660 to 680 cm^{-1} has been measured in gas phase and in inert matrices.²⁶ This difference translates into about 4 kJ/mol in the ΔH^\ddagger value, which is within the experimental uncertainty equal to $E_a(\text{D}_2\text{O}) - E_a(\text{H}_2\text{O}) = 5.1 \pm 1.3$ kJ/mol from Table 1.

The energy splitting of the adiabatic surfaces in Figure 4 is mainly due to the spin–orbit interactions and may conceivably be insufficient for a facile singlet–triplet transition in the activated complex. In this case, the precursor complex will have to proceed along the singlet energy surface all the way up to the formation of discrete ${}^1\text{NO}^-$ species. Such a mechanism involving equilibrium formation of ${}^1\text{NO}^-$ in reaction 4 and its subsequent radiationless transition to ${}^3\text{NO}^-$ via reaction 8 is shown in Scheme 3.

For this mechanism

$$k_2 = \frac{k_8}{K_4} = A_8 \exp\left(-\frac{\Delta_{r4}S^0}{R}\right) \exp\left(-\frac{E_8 - \Delta_{r4}H^0}{RT}\right) \quad (15)$$

where A_8 and E_8 are Arrhenius parameters for reaction 8 and $\Delta_{r4}S^0$ and $\Delta_{r4}H^0$ are entropy and enthalpy changes in reaction 4. As with the ${}^1\text{O}_2({}^1\Delta_g) \rightarrow {}^3\text{O}_2({}^3\Sigma_g^-)$ transition^{27–29} and with most $S \rightarrow T$ transitions,²¹ reaction 8 is unlikely to be significantly activated, so we may expect that $E_8 \approx 0$. The value of $\Delta_{r4}S^0$ is unknown, but is expected to be relatively small by analogy with CN^- and ClO^- , for which entropy changes in protonation by water are estimated as -50 and $+19$ J/(mol K), respectively, from the NBS tables.¹⁹ By setting $\Delta_{r4}S^0 = 0$, parameters in eq 15 can be connected with experimental values in Table 1, that is $E_a = -\Delta_{r4}H^0 = -\Delta_{r4}G^0$ and $\log(A_2) = \log(A_8) = \log(k_8)$, in proper units. Thus, reaction 8 must be about 4 orders of magnitude more rapid than deactivation of ${}^1\text{O}_2({}^1\Delta_g)$ ³⁰ and hence belongs among the fastest $S \rightarrow T$ transitions.²¹ There are at least three factors that can facilitate deactivation of ${}^1\text{NO}^-$ compared to ${}^1\text{O}_2$. First, the singlet–triplet energy splitting is roughly 25 kJ/mol smaller. Second, the interaction between ${}^1\text{NO}^-$ and water should be stronger and more symmetry-breaking, particularly due to hydrogen bonding; interactions with a solvent are known to play a pivotal role in the radiationless deactivation of ${}^1\text{O}_2$.^{31–34} Third, the symmetry of NO^- is lower, so that there are no parity

restrictions associated with g parity of the electronic states in O_2 . If indeed $k_8 \approx 1 \times 10^{10} \text{ s}^{-1}$, then k_4 will have to be about $2.5 \times 10^{11} \text{ s}^{-1}$ (eq 13), a perfectly reasonable value for a barrierless, exergonic, proton-transfer reaction with a hydrogen-bonded solvent.

A substantially negative $\Delta_{r4}S^0$ will make k_8 more ordinary, but it will also increase $-\Delta_{r4}G^0$ that is already too high, even with $\Delta_{r4}S^0 = 0$. Indeed, the value of $-\Delta_{r4}G^0 = 53$ kJ/mol from Figure 4 is 23 kJ/mol larger than E_a in Table 1, which would disprove the mechanism, if the energetics of nitroxyl species were precisely established. However, this is not the case and the most significant uncertainty concerns the energy gap between ${}^1\text{NO}^-$ and ${}^3\text{NO}^-$ that was taken from the gas-phase measurements by Tronc and co-workers.³⁵ They noted that their measurements could possibly pertain to the first vibrationally excited level of ${}^1\text{NO}^-$ that is 18 kJ/mol above the zero-point energy. If so, the value $-\Delta_{r4}G^0$ would decrease to about 35 kJ/mol and become sufficiently close to the observed E_a , considering other uncertainties in nitroxyl energetics in water. Graphically, this re-evaluation of $-\Delta_{r4}G^0$ would correspond to bringing down the ${}^1\text{NO}^- + \text{H}_2\text{O}$ level in Figure 4 almost to the shown singlet–triplet intersection point; it would also lower $pK_a({}^1\text{HNO}/{}^1\text{NO}^-)$ from about 23 to approximately 20. Both numbers are within the uncertainty margins of recent ab initio estimate for this pK_a .⁸

In terms of eq 15, the kinetic isotope effect depends on 3 ratios

$$\text{KIE} = \frac{K_4^D k_8^H}{K_4^H k_8^D} = \frac{K_a^H K_w^D k_8^H}{K_a^D K_w^H k_8^D} \quad (16)$$

where superscripts H and D mark values for normal and heavy water, K_w is the ionic product of water, and K_a is the acid dissociation constant for ${}^1\text{HNO} = {}^1\text{NO}^- + \text{H}^+$. The ratio $K_a^H/K_a^D \approx 6.5$ can be estimated from the well-behaved relationship $\log(K_a^H/K_a^D) = 0.41 + 0.02pK_a^H$ described by Bell³⁶ and the ratio $K_w^D/K_w^H \approx 0.15$ has been measured.³⁷ To account for the observed KIE, the ratio k_8^H/k_8^D will have to be about 3.2, not too dissimilar from the corresponding ratio of 13–16 for singlet oxygen.^{30,38} We thus conclude, that the mechanism in Scheme 3 is also consistent with the observations, provided that the exothermicity of reaction 4 is about 20 kJ/mol lower than it has been estimated previously.⁷

Although more accurate knowledge of the nitroxyl energetics is required to cleanly discriminate the pathways shown in Schemes 2 and 3, we should point out that these mechanisms are, in fact, conceptually very similar. In both cases, the spin prohibition demands significant activation before spin change can take place, but the spin change itself must occur extremely rapidly once it has become energetically allowed. In other words, if both energy levels for the ${}^3\text{NO}^- + \text{H}_2\text{O}$ and ${}^1\text{NO}^- + \text{H}_2\text{O}$ products in Figure 4 were some 50–70 kJ/mol lower, the

(25) Creutz, C.; Sutin, N. *J. Am. Chem. Soc.* **1988**, *110*, 2418–2427.

(26) Jacox, M. E. *J. Phys. Chem. Ref. Data* **1988**, *17*, 269–512.

(27) Ogilby, P. R.; Foote, C. S. *J. Am. Chem. Soc.* **1983**, *105*, 3423–3430.

(28) Zinukov, S. V.; Kamalov, V. F.; Koroteev, N. I.; Krasnovsky, A. A., Jr. *Opt. Spectrosc. (USSR)* **1991**, *70*, 460–462.

(29) Bisby, R. H.; Morgan, C. G.; Hamblett, I.; Gorman, A. A. *J. Phys. Chem. A* **1999**, *103*, 7454–7459.

(30) Rodgers, M. A. J.; Snowden, P. T. *J. Am. Chem. Soc.* **1982**, *104*, 5541–5543.

(31) Merkel, P. B.; Kearns, D. R. *J. Am. Chem. Soc.* **1972**, *94*, 7244–7253.

(32) Hurst, J. R.; Schuster, G. B. *J. Am. Chem. Soc.* **1983**, *105*, 5756–5760.

(33) Rodgers, M. A. J. *J. Am. Chem. Soc.* **1983**, *105*, 6201–6205.

(34) Schmidt, R.; Brauer, H.-D. *J. Am. Chem. Soc.* **1987**, *109*, 6976–6981.

(35) Tronc, M.; Huetz, A.; Landau, M.; Pichou, F.; Reinhardt, J. *J. Phys. B* **1975**, *8*, 1160–1169.

(36) Bell, R. P. *The Proton in Chemistry*; Cornell University Press: Ithaca, New York, 1959.

(37) Kingerley, R. W.; LaMer, V. K. *J. Am. Chem. Soc.* **1941**, *63*, 3256–3262.

(38) Schmidt, R.; Afshari, E. *Ber. Bunsen-Ges. Phys. Chem.* **1992**, *96*, 788–794.

activation barrier would disappear and the spin-forbidden reaction 2 would proceed at nearly diffusion-controlled rate, like a spin-allowed reaction. Similarly, if the energy levels remained the same, but the ground/excited-state multiplicities of NO^- were reversed, the reaction would again be diffusion-controlled. Thus, we conclude that a synergy between the spin prohibition and energetics creates what can be called an "intersystem barrier" and is responsible for slowness of the spin-forbidden deprotonation of ${}^1\text{HNO}$ by OH^- ; the spin prohibition alone plays a minor role. The activation parameters in Table 1 clearly attest to these points.

Acknowledgment. We thank Drs. Marshall Newton, Harold Schwarz, and Norman Sutin for insightful discussions. Work at New York University was supported by the NIH Grant No. 1R01 ES1189-01 and by a grant from the Kresge Foundation. Research at Brookhaven National Laboratory was carried out under the auspices of the U.S. Department of Energy under Contract No. DE-AC02-98CH10886 from the Division of Chemical Sciences, Office of Basic Energy Sciences.<http://pubs.acs.org>.

JA034378J